


**Closed-form modeling of neuronal spike train statistics using multivariate Hawkes cumulants**Nicolas Privault  and Michèle Thieullen*Division of Mathematical Sciences, School of Physical and Mathematical Sciences, Nanyang Technological University, 21 Nanyang Link, Singapore 637371, Singapore  
and LPSM - UMR 8001, Sorbonne Université, 4 Place Jussieu, 75252 Paris, France*

(Received 14 February 2022; revised 24 September 2022; accepted 27 October 2022; published 17 November 2022)

We derive exact analytical expressions for the cumulants of any orders of neuronal membrane potentials driven by spike trains in a multivariate Hawkes process model with excitation and inhibition. Such expressions can be used for the prediction and sensitivity analysis of the statistical behavior of the model over time and to estimate the probability densities of neuronal membrane potentials using Gram-Charlier expansions. Our results are shown to provide a better alternative to Monte Carlo estimates via stochastic simulations and computer codes based on combinatorial recursions are included.

DOI: [10.1103/PhysRevE.106.054410](https://doi.org/10.1103/PhysRevE.106.054410)**I. INTRODUCTION**

Hawkes processes [1] are self-exciting point processes that have been applied to the modeling of random spike trains in neuroscience in, e.g., Refs. [2–5]. Neuronal spike train activity has been modeled using multivariate Hawkes processes in, e.g., Refs. [6–8], where filtered Hawkes processes have been interpreted as free membrane potentials in the linear-nonlinear cascade model. In this framework, the cumulants of multivariate Hawkes processes yield important statistical information. However, the analysis of statistical properties of Hawkes processes is made difficult by their recursive nature, in particular, computing the cumulants of Hawkes processes involves technical difficulties due to the infinite recursions involved.

Neuronal synaptic input has also been modeled using multiplicative Poisson shot noise driven by random current spikes, in, e.g., Refs. [9,10], see also [11–14], for the analysis of stationary limits in the case of constant Poisson arrival rates, and [15,16], see also [17–19], for time-dependent Poisson intensities modeling of time-inhomogeneous synaptic input. In this framework, the time evolution of the probability density functions of membrane potentials has been described in [20,21] by Gram-Charlier probability density expansions based on moment and cumulant estimates.

The computation of the moments of Hawkes processes has been the object of several approaches, see [22–24] for the use of differential equations and [25] for stochastic calculus methods applied to first and second order moments. Other techniques have been introduced for linear and nonlinear self-exciting processes, including Feynman diagrams [7], path integrals [8], and tree-based methods [26] applied up to third order cumulants. However, such methods appear difficult to implement systematically for higher order cumulants and they use finite order expansions that only approximate cumulants even in the linear case.

In this paper, we provide a recursion for the closed-form computation of the cumulants of multivariate Hawkes processes, without involving approximations. For this, we extend

the recursive algorithm of [27] to the computation of joint cumulants of all orders of multivariate Hawkes processes. This algorithm, based on a recursive relation for the probability generating function (PGF) of self-exciting point processes started from a single point, relies on sums over partitions and Bell polynomials. In what follows, we will apply this algorithm to Hawkes processes with inhibition, by using negative weights in their cluster point process construction. We note that although our cumulant expressions are proved only for non-negative weights, the results remain numerically accurate and consistent with the sampled cumulants of Hawkes processes with inhibition as long as the process does not become inactive over long time intervals; see also Sec. 1 of [7].

In Proposition 1 and Corollary 2 we compute the joint cumulants of membrane potentials modeled according to a filtered Hawkes process as in [7]. In comparison with Monte Carlo simulation estimates, explicit expressions allow for immediate numerical evaluations over multiple ranges of parameters, whereas Monte Carlo estimations can be slow to implement. In addition, such expressions are suitable for algebraic manipulations and tabulation, e.g., they can be differentiated in closed form with respect to time to yield the dynamics of cumulants or with respect to any system parameter to yield sensitivity measures. Numerical applications of our closed form expressions are presented in Sec. III, where they are compared to Monte Carlo estimates. Although our simulations in Figs. 3–10 have been run with 10 million samples, Monte Carlo estimates of higher-order cumulants can be subject to numerical instabilities not observed with closed-form expressions. In particular, they become degraded starting with joint third cumulants (see Fig. 8) and fourth cumulants (see Fig. 9), and they become clearly insufficient for the estimation of fourth joint cumulants (see Fig. 10).

Closed-form cumulant expressions are then applied in Sec. IV to the explicit derivation of cumulant-based Gram-Charlier expansions for the probability density function of the membrane potentials at any given time, showing that densities are negatively skewed with positive excess kurtosis.

We proceed as follows. In Sec. II we present closed-form recursions for the computation of cumulants of any order in a multivariate Hawkes process model. Numerical results are then presented in Sec. III with application to the modeling of connectivity in spike train statistics. In Sec. IV we present numerical experiments based on cumulants for the estimation of probability densities of potentials by Gram-Charlier expansions. In the Appendixes we present the derivation of recursive cumulant and moment identities for the closed-form computation of the moments of Hawkes processes, in the multivariate case, with the corresponding codes written in MAPLE and MATHEMATICA.

**II. CUMULANTS OF MULTIVARIATE HAWKES PROCESSES**

This section describes our algorithm for the computation of cumulants. Let  $[H_1(t), \dots, H_n(t)]_{t \geq 0}$  denote a multivariate linear Hawkes point process with self-exciting stochastic intensities of the form

$$\lambda_i(t) := v_i(t) + \sum_{j=1}^n \int_0^t \gamma_{i,j}(t-s) dH_j(s), \quad t \in \mathbb{R}_+, \quad (1)$$

with Poisson offspring intensities  $\gamma_{i,j}(dx) = \gamma_{i,j}(x)dx$  and possibly time inhomogeneous Poisson baseline intensities  $v_i(dt) = v_i(t)dt$ ,  $i = 1, \dots, m$ . The next proposition provides a way to compute the joint cumulants of random sums by an induction relation based on the Bell polynomials. In what follows, we assume that  $\gamma_1(\mathbb{R}_+) + \dots + \gamma_m(\mathbb{R}_+) < 1$ , and consider the integral operator  $\Gamma$  defined as

$$(\Gamma f)(x, i) = \sum_{j=1}^m \int_0^\infty f(x+y, j) \gamma_{i,j}(dy),$$

with  $x \in \mathbb{R}_+$ ,  $i = 1, \dots, m$ , and, letting  $I$  denote identity, the inverse operator  $(I - \Gamma)^{-1}$  given by

$$\begin{aligned} [(I - \Gamma)^{-1} f](x, i) &= f(x, i) + \sum_{n=1}^\infty (\Gamma^n f)(x, i) \\ &= f(x, i) + \sum_{n=1}^\infty \sum_{j_1, \dots, j_n=1}^m \int_0^\infty \dots \int_0^\infty \\ &\quad \times f(x + y_1 + \dots + y_n, j_n) \gamma_{i, j_1}(dy_1) \dots \gamma_{j_{n-1}, j_n}(dy_n), \end{aligned}$$

with  $x \in \mathbb{R}_+$ ,  $i = 1, \dots, m$ . The following statements hold for the joint cumulants  $\kappa_{(x,i)}^{(n)}(f_1, \dots, f_n)$  of  $(\sum_{j=1}^m \int_0^\infty f_i(t, j) dH_j(t), \dots, \sum_{j=1}^m \int_0^\infty f_n(t, j) dH_j(t))$ , given that the multidimensional Hawkes process is started from a single jump located in  $H_i(t)$  at time  $x \in \mathbb{R}_+$ ,  $i = 1, \dots, m$ .

*Proposition 1.* (1) The first cumulant  $\kappa_{(x,i)}^{(1)}(f)$  of  $\sum_{j=1}^m \int_0^\infty f(t, j) dH_j(t)$  is given by

$$\begin{aligned} \kappa_{(x,i)}^{(1)}(f) &= [(I - \Gamma)^{-1} f](x, i) \\ &= f(x, i) + \sum_{n=1}^\infty \sum_{j_1, \dots, j_n=1}^m \int_0^\infty \dots \int_0^\infty \\ &\quad \times f(x + y_1 + \dots + y_n, j_n) \gamma_{i, j_1}(dy_1) \dots \gamma_{j_{n-1}, j_n}(dy_n), \end{aligned}$$

with  $x \geq 0$ ,  $i = 1, \dots, m$ .

For  $n \geq 2$ , the joint cumulants  $\kappa_{(x,i)}^{(n)}(f_1, \dots, f_n)$  are given by the induction relation

$$\begin{aligned} \kappa_{(x,i)}^{(n)}(f_1, \dots, f_n) &= \sum_{k=2}^n \sum_{\pi_1 \cup \dots \cup \pi_k = \{1, \dots, n\}} \\ &\quad \times \left( (I - \Gamma)^{-1} \Gamma \prod_{j=1}^k \kappa_{(\cdot, \cdot)}^{(|\pi_j|)}[(f_l)_{l \in \pi_j}] \right)(x, i), \quad (2) \end{aligned}$$

with  $x \geq 0$ ,  $i = 1, \dots, m$ ,  $n \geq 2$ , where the above sum is over set partitions  $(\pi_1, \dots, \pi_k)$  of  $\{1, \dots, n\}$  and  $|\pi_i|$  denotes the cardinality of the set  $\pi_i$ ,  $i = 1, \dots, k$ .

*Proof.* See Appendix A.

Standard (i.e., unconditional) cumulants can then be obtained in the next corollary as a consequence of Proposition 1.

(2) *Corollary 2.* The joint cumulants  $\kappa^{(n)}(f_1, \dots, f_n)$  of  $(\sum_{j=1}^m \int_0^\infty f_i(t, j) dH_j(t))_{1 \leq i \leq n}$  are given by the relation

$$\begin{aligned} \kappa^{(n)}(f_1, \dots, f_n) &= \sum_{i=1}^m \sum_{k=1}^n \sum_{\pi_1 \cup \dots \cup \pi_k = \{1, \dots, n\}} \int_0^\infty \prod_{j=1}^k \kappa_{(x,i)}^{(|\pi_j|)}[(f_l)_{l \in \pi_j}] v_i(x) dx, \quad (3) \end{aligned}$$

with  $n \geq 1$ .

*Proof.* See Appendix A.

**A. Exponential kernels**

Joint cumulants will be computed using sums over partitions and Bell polynomials in the case of the exponential offspring intensities

$$\gamma_{i,j}(dx) = w_{i,j} \mathbf{1}_{[0, \infty)}(x) e^{-bx} dx, \quad i, j = 1, \dots, m,$$

given by the  $m \times m$  connectivity matrix  $W = (w_{i,j})_{1 \leq i, j \leq m}$ ,  $|w_{i,j}| < b$ , and the constant Poisson intensities  $v_i(dz) = v_i dz$ ,  $v_i > 0$ ,  $i, j = 1, \dots, m$ . In this case, the integral operator  $\Gamma$  satisfies

$$(\Gamma f)(x, i) = \sum_{j=1}^m w_{i,j} \int_0^\infty f(x+y, j) e^{-by} dy,$$

with  $x \in \mathbb{R}_+$ ,  $i = 1, \dots, m$ . The recursive calculation of joint cumulants can be performed using the family of functions  $e_{p, \eta, t, j}(x, i) := \mathbf{1}_{\{i=j\}} x^p e^{\eta x} \mathbf{1}_{[0, t]}(x)$ ,  $\eta < b$ ,  $p \geq 0$ , by evaluating  $(I - \Gamma)^{-1} \Gamma$  in Proposition 1 on the family of functions  $e_{p, \eta, t, j}$  as in the next lemma.

*Lemma 3.* For  $f$  in the linear span generated by the functions  $e_{p, \eta, t, k}$ ,  $p \geq 0$ ,  $\eta < b$ ,  $k = 1, \dots, m$ , the operator  $(I - \Gamma)^{-1} \Gamma$  is given by

$$[(I - \Gamma)^{-1} \Gamma f](x, i) = \sum_{j=1}^m \int_0^{t-x} f(x+y, j) [W e^{yW}]_{i,j} e^{-by} dy,$$

with  $x \in [0, t]$ ,  $i = 1, \dots, m$ .

For  $f$  as in Lemma 3, by Proposition 1 the first cumulant of  $\sum_{j=1}^m \int_0^\infty f_i(t, j) dH_j(t)$  given that the multidimensional Hawkes

process is started from a single jump located in  $H_i(t)$  at time  $x \in \mathbb{R}_+, i = 1, \dots, m$ , is given by

$$\kappa_{(x,i)}^{(1)}[f(\cdot)\mathbf{1}_{\{j\}}] = f(x)\mathbf{1}_{\{i=j\}} + \int_0^{t-x} e^{-by} f(x+y)[W e^{yW}]_{i,j} dy,$$

with  $x \in [0, t], i = 1, \dots, m$ , and for  $n \geq 2$  we have the recursion

$$\begin{aligned} \kappa_{(x,i)}^{(n)}(f\mathbf{1}_{[0,t]}) &= \sum_{k=2}^n \sum_{j=1}^m \int_0^{t-x} e^{-by} [W e^{yW}]_{i,j} \\ &\quad \times B_{n,k}[\kappa_{(x+y,j)}^{(1)}(f), \dots, \kappa_{(x+y,j)}^{(n-k+1)}(f)] dy. \end{aligned}$$

The conditional multivariate joint cumulants of  $[\int_0^\infty f_i(t, j_i) dH_{j_i}(t)]_{1 \leq i \leq n}$  are given by

$$\begin{aligned} \kappa_{(x,i)}^{(n)}(f_1\mathbf{1}_{[0,t_1]}\mathbf{1}_{\{j_1\}}, \dots, f_n\mathbf{1}_{[0,t_n]}\mathbf{1}_{\{j_n\}}) \\ &= \sum_{j=1}^m \sum_{k=2}^n \sum_{\pi_1 \cup \dots \cup \pi_k = \{1, \dots, n\}} \\ &\quad \times \int_0^{\min(t_1, \dots, t_m) - x} e^{-by} [W e^{yW}]_{i,j} \\ &\quad \times \prod_{l=1}^k \kappa_{(x+y, j)}^{(|\pi_l|)} [(f_p \mathbf{1}_{\{j_p\}})_{p \in \pi_l}] dy, \end{aligned}$$

where  $j_1, \dots, j_n \geq 1$ , with, for  $n = 2$ ,

$$\begin{aligned} \kappa_{(x,i)}^{(2)}(f_1\mathbf{1}_{[0,t_1]}\mathbf{1}_{\{j_1\}}, f_2\mathbf{1}_{[0,t_2]}\mathbf{1}_{\{j_2\}}) &= \sum_{j=1}^m \int_0^{\min(t_1, t_2) - x} \\ &\quad \times e^{-by} [W e^{yW}]_{i,j} \kappa_{(x+y, j)}^{(1)}(f_1\mathbf{1}_{\{j_1\}}) \kappa_{(x+y, j)}^{(1)}(f_2\mathbf{1}_{\{j_2\}}) dy. \end{aligned}$$

### III. NUMERICAL EXAMPLES

We consider a nonlinear multivariate Hawkes process  $[\tilde{H}_1(t), \dots, \tilde{H}_m(t)]_{t \in \mathbb{R}_+}$  with intensities

$$\tilde{\lambda}_i(t) := \left( v_i(t) + \sum_{j=1}^n \int_0^t \gamma_{i,j}(t-s) d\tilde{H}_j(s) \right)^+, \quad (4)$$

$t \in \mathbb{R}_+$ , with exponential offspring intensities

$$\gamma_{i,j}(dx) = w_{i,j} \mathbf{1}_{[0, \infty)}(x) e^{-bx} dx, \quad i, j = 1, \dots, m,$$

where  $(w_{i,j})_{1 \leq i, j \leq m}$  is a matrix of synaptic weights which are possibly negative due to inhibition. The inputs

$$v_i(t) + \sum_{j=1}^n \int_0^t \gamma_{i,j}(t-s) d\tilde{H}_j(s), \quad i = 1, \dots, m,$$

have been interpreted in [7] as a family of free neuronal membrane potentials, which have the ability to directly influence the underlying spike rate.

In this paper, we model the membrane potentials  $V_i(t)$  using the filtered processes

$$V_i(t) = \int_0^t g_i(t-s) dH_i(s), \quad t \in \mathbb{R}_+, \quad i = 1, \dots, m,$$

where  $[H_1(t), \dots, H_n(t)]_{t \geq 0}$  is the multivariate linear Hawkes process defined in (1) and  $g_i(t)$  are impulse response functions

such that  $g_i(u) = 0$  for  $u < 0, i, j = 1, \dots, m$ . We assume that the kernel  $g_i(t)$  takes the form

$$g_i(t) := \mathbf{1}_{[0, \infty)}(t) e^{-t/\tau_s}, \quad i = 1, \dots, m, \quad t \in \mathbb{R}.$$

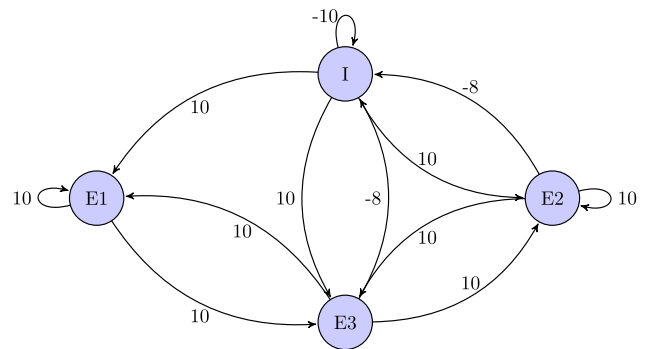
We note that although Proposition 1 and Corollary 2 are only proved for  $[H_1(t), \dots, H_m(t)]_{t \in \mathbb{R}_+}$  with non-negative weights in the cluster process framework of [28], the results remain numerically accurate and consistent with the sampled cumulants of (4), provided that the inhibitory weights  $w_{i,j}$  do not become too negative; see Sec. 1 of [7].

Our cumulant expressions are compared to the sampled cumulants of the nonlinear Hawkes process  $[\tilde{H}_1(t), \dots, \tilde{H}_m(t)]_{t \in \mathbb{R}_+}$  in (4) in the presence of negative weights. The joint cumulant  $\langle\langle V_{l_1}(t_1) \cdots V_{l_n}(t_n) \rangle\rangle, 1 \leq l_1, \dots, l_n \leq m$ , is evaluated in closed form by induction by the command `c(W, b, [g, ..., g], [l1, ..., ln], [t1, ..., tn])` in MAPLE or `c[W, b, g, ..., g, l1, ..., ln, t1, ..., tn]` in MATHEMATICA, defined in the code blocks presented in Appendix B. Closed form expressions for higher order joint moments and cumulants may involve thousands of terms resulting of symbolic computations in MAPLE or MATHEMATICA; nevertheless, their numerical implementation remains attractive in terms of computation time and stability properties.

In the following numerical examples we take  $m = 4$  and consider the potentials  $[V_1(t), V_2(t), V_3(t), V_4(t)] = [V_{E1}(t), V_{E2}(t), V_{E3}(t), V_I(t)]$ , with three excitatory neurons and one inhibitory neuron, parametrized by the weight matrix

$$W = (w_{i,j})_{1 \leq i, j \leq 4} = \begin{matrix} & \begin{matrix} E1 & E2 & E3 & I \end{matrix} \\ \begin{matrix} E1 \\ E2 \\ E3 \\ I \end{matrix} & \begin{pmatrix} 10 & 0 & 10 & 0 \\ 0 & 10 & 10 & -8 \\ 10 & 10 & 0 & -8 \\ 10 & 10 & 10 & -10 \end{pmatrix} \end{matrix}.$$

Note that this example does not have resetlike effects. Although this example is restricted to four neurons for the sake of computation time, the algorithm is valid for any  $m \geq 1$ . The connectivity of the network can be represented as follows:



Figures 1 and 2 present random simulations of the membrane potentials  $V_{E2}(t)$  and  $V_{E4}(t)$  with  $T = 0.1$  s with  $g(u) = e^{-u/\tau_s} \mathbf{1}_{[0, \infty)}(u)$ , with  $b = 50$  Hz,  $\tau_s = 0.01$  s, and  $v_i = 250$  Hz,  $i = 1, 2, 3, 4$ . We use the algorithm of [29] for the simulation of multivariate Hawkes processes, and its implementation given in [30].

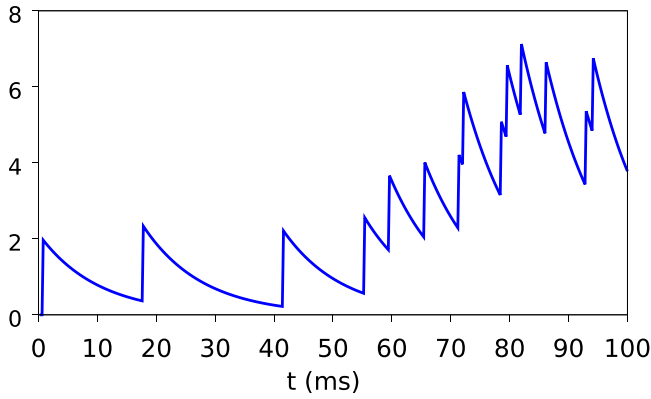


FIG. 1. Excitatory potential  $V_2(t) = V_{E2}(t)$ .

The following Figs. 3–10 present numerical cumulant estimates using closed form expression and compare them with Monte Carlo simulations run with 10 million samples. Figures 3 and 4 present numerical estimates of first moment and standard deviation, together with the mean obtained by Monte Carlo simulations.

Figures 3–6 can be obtained from the MAPLE commands listed below together with their run times on a standard laptop computer, after loading the function definitions listed in Appendix B and the variable assignments of  $W$  and  $\mu$ :

```

W := <<10, 0, 10, 10> | <0, 10, 10, 10> | <10, 10, 0, 10> |
    <0, -8, -8, -10>>;
mu := [t -> 250, t -> 250, t -> 250, t -> 250]; g := (x, t)
    -> exp(-100*t + 100*x);
c(W, 50, [g], [2], [t], mu) # First cumulant of V2(t) -
    comp. time one second
c(W, 50, [g,g], [4,4], [t,t], mu) # Second cumulant of V4(t)
    - comp. time 7 seconds
c(W, 50, [g,g], [4,2], [t,0.05], mu) # Covariance of
    (V2(t1),V4(t)) for t<t1=0.05 - comp. time 12 seconds
c(W, 50, [g,g], [2,4], [0.05,t], mu) # Covariance of
    (V2(t1),V4(t)) for t>t1=0.05 - comp. time 15 seconds
    
```

Figures 5 and 6 present estimates of the cross correlations  $\text{Cor}[V_{E2}(t), V_{E4}(t)]$  and  $\text{Cor}[V_{E2}(t_1), V_1(t)]$  with  $t_1 := 50$  ms and  $t \in [0, 100]$  ms].

Figures 7 and 8 present time-dependent estimates of the third cumulant of  $V_1(t)$  and third joint cumulant of  $[V_{E1}(t_1), V_{E1}(t_1), V_1(t)]$  with  $t_1 = 0.05$ , based on the exact moment expressions

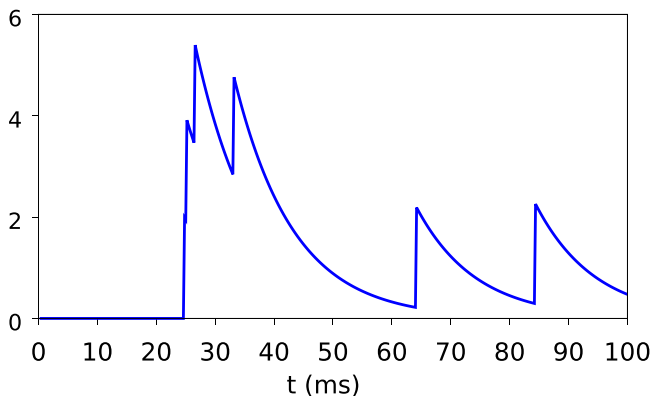


FIG. 2. Inhibitory potential  $V_4(t) = V_1(t)$ .

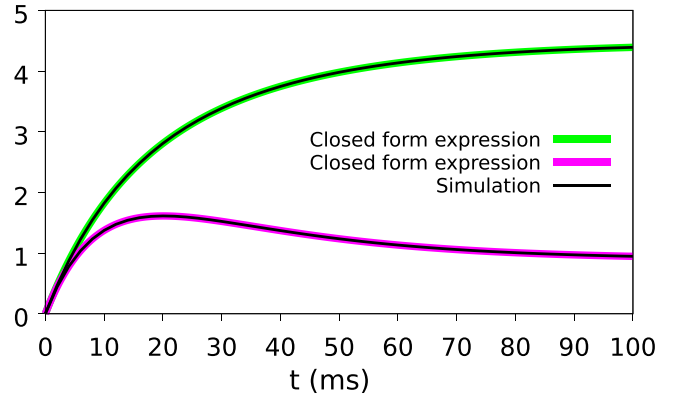


FIG. 3. Means of  $V_2(t) = V_{E2}(t)$  and  $V_4(t) = V_1(t)$ .

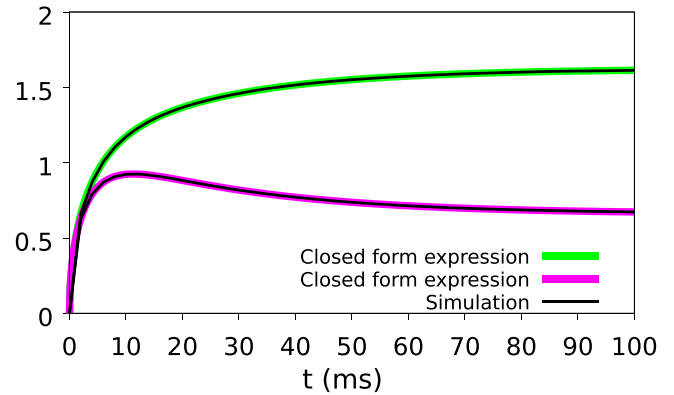


FIG. 4. Standard deviations of  $V_{E2}(t)$  and  $V_1(t)$ .

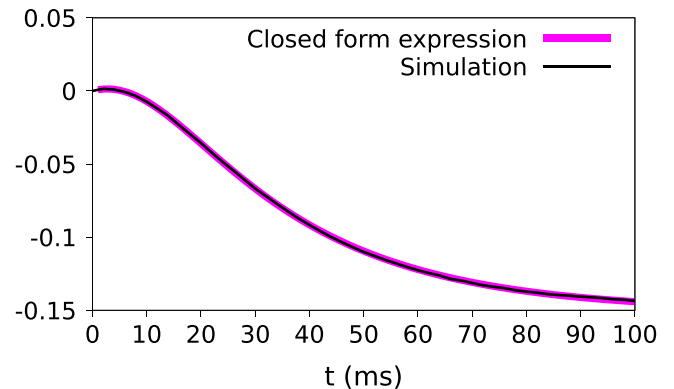


FIG. 5. Cross correlation of  $[V_{E2}(t), V_1(t)]$ .

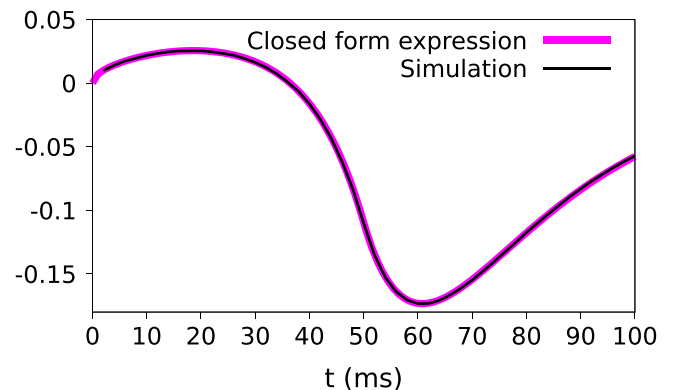


FIG. 6. Cross correlation of  $[V_{E2}(t_1), V_1(t)]$ .

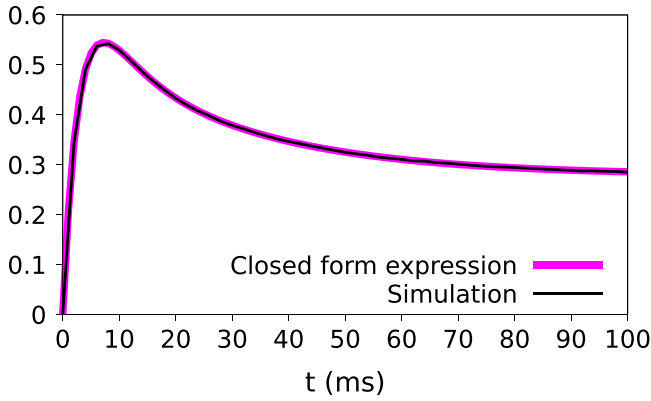


FIG. 7. Third cumulant of  $V_4(t) = V_1(t)$ .

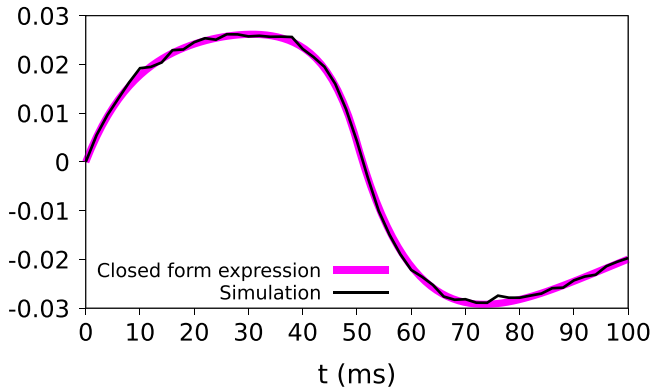


FIG. 8. Joint cumulant of  $[V_{E1}(t_1), V_{E1}(t_1), V_1(t)]$ .

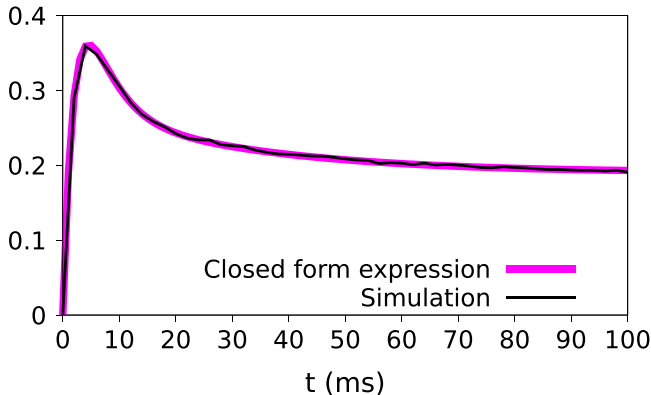


FIG. 9. Fourth cumulant of  $V_4(t) = V_1(t)$ .

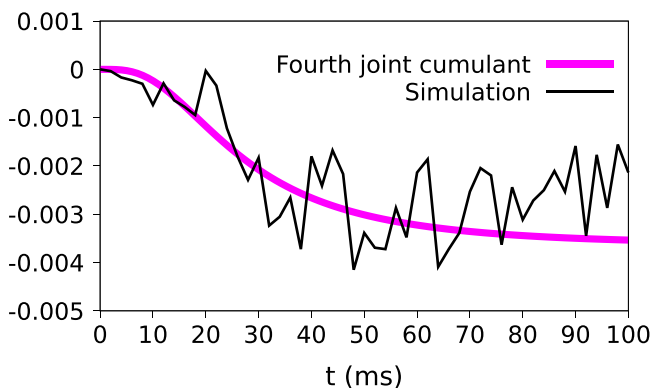


FIG. 10. Joint cumulant of  $[V_{E1}(t), \dots, V_{E3}(t), V_1(t)]$ .

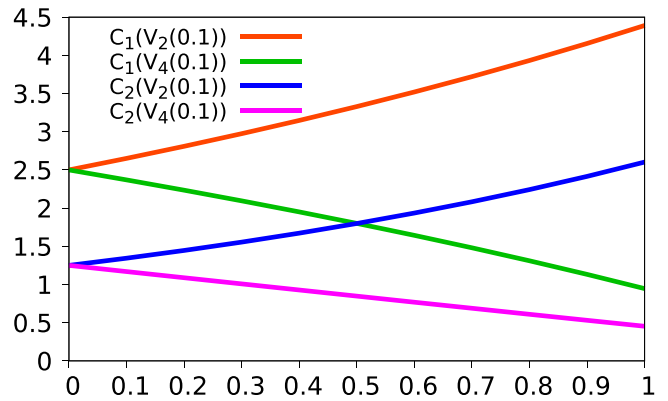


FIG. 11. Sensitivities of first and second cumulants.

computed in MAPLE by the following commands:

```
c(W, 50, [g,g,g], [4,4,4], [t,t,t], mu) # Third cumulant of
V4(t) - comp. time 56 seconds
c(W, 50, [g,g,g], [4,1,1], [t,0.05,0.05], mu) # Third joint
cumulant of (V1(t1),V1(t1),V4(t)), t<t1=0.05 - comp.
time 239 seconds
c(W, 50, [g,g,g], [1,1,4], [0.05,0.05,t], mu) # Third joint
cumulant of (V1(t1),V1(t1),V4(t)), t>0.05 - comp. time
473 seconds
```

Figures 9 and 10 present estimates of the fourth cumulant of  $V_1(t)$  and of the fourth joint cumulant of  $[V_{E1}(t), V_{E2}(t), V_{E3}(t), V_1(t)]$  respectively, computed by the following commands:

```
c(W, 50, [g,g,g,g], [4,4,4,4], [t,t,t,t], mu) # 4th cumulant
of V4(t) - comp. time 677 seconds
c(W, 50, [g,g,g,g], [1,2,3,4], [t,t,t,t], mu) # 4th joint
cumulant of (V1(t),V2(t),V3(t),V4(t)) - comp. time
14917 seconds
```

One can check from Figs. 8 and 10 that the precision of Monte Carlo estimation is degraded starting with joint third cumulants and fourth cumulants, while it becomes clearly insufficient for an accurate estimation of fourth joint cumulants in Fig. 10. This phenomenon has also been observed in [21] when modeling neuronal activity using Poisson processes and can be attributed to the fact that the estimation of fourth-order joint cumulants in terms of sampled moments involves a multinomial expression of order four in four variables with changing signs.

The knowledge of cumulants in explicit form also allows us to study their behavior under the variation of other parameters. In Figs. 11 and 12 we plot the respective evolutions of the first four cumulants of  $V_{E2}(0.1)$  and  $V_1(0.1)$  as a function of  $\alpha W$  with  $\alpha \in [0, 1]$ .

#### IV. GRAM-CHARLIER EXPANSIONS

In this section we use our cumulant formulas for the estimation of probability densities of potentials by Gram-Charlier expansions. The Gram-Charlier expansion of the continuous probability density function  $\phi_X(x)$  of a random variable  $X$  is given by

$$\phi_X(x) = \frac{1}{\sqrt{\kappa_2}} \varphi\left(\frac{x - \kappa_1}{\sqrt{\kappa_2}}\right) + \frac{1}{\sqrt{\kappa_2}} \sum_{n=3}^{\infty} c_n H_n\left(\frac{x - \kappa_1}{\sqrt{\kappa_2}}\right) \varphi\left(\frac{x - \kappa_1}{\sqrt{\kappa_2}}\right), \quad (5)$$

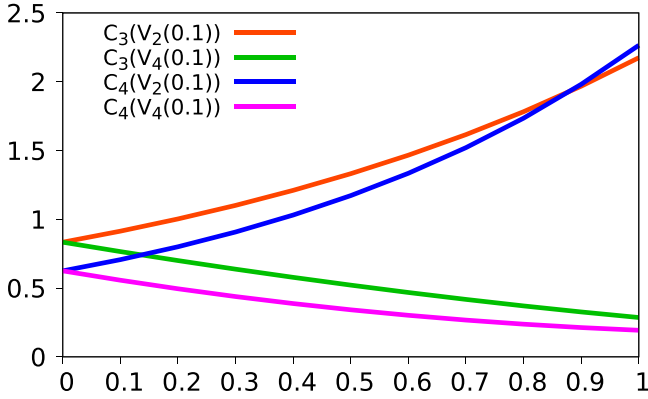


FIG. 12. Sensitivities of third and fourth cumulants.

see Sec. 17.6 of [31], where (i)  $\varphi(x) := \frac{1}{\sqrt{2\pi}}e^{-x^2/2}$ ,  $x \in \mathbb{R}$ , is the standard normal density function, (ii)  $H_n(x) := \frac{(-1)^n}{\varphi(x)} \frac{\partial^n \varphi}{\partial x^n}(x)$ ,  $x \in \mathbb{R}$ , is the Hermite polynomial of degree  $n \geq 0$ , with  $H_0(x) = 1$ ,  $H_1(x) = x$ ,  $H_3(x) = x^3 - 3x$ ,  $H_4(x) = x^4 - 6x^2 + 3$ , and  $H_6(x) = x^6 - 15x^4 + 45x^2 - 15$ , and (iii) the sequence  $(c_n)_{n \geq 3}$  is given from the cumulants  $(\kappa_n)_{n \geq 1}$  of  $X$  as

$$c_n = \frac{1}{(\kappa_2)^{n/2}} \sum_{m=1}^{[n/3]} \sum_{\substack{l_1 + \dots + l_m = n \\ l_1, \dots, l_m \geq 3}} \frac{\kappa_{l_1} \dots \kappa_{l_m}}{m! l_1! \dots l_m!}, \quad n \geq 3.$$

In particular,  $c_3$  and  $c_4$  can be expressed from the skewness  $\kappa_3/(\kappa_2)^{3/2}$  and the excess kurtosis  $\kappa_4/(\kappa_2)^2$ , with

$$c_3 = \frac{\kappa_3}{3!(\kappa_2)^{3/2}}, \quad c_4 = \frac{\kappa_4}{4!(\kappa_2)^2},$$

$$c_5 = \frac{\kappa_5}{5!\kappa_5^{5/2}}, \quad c_6 = \frac{\kappa_6}{6!(\kappa_2)^3} + \frac{(\kappa_3)^2}{2(3!)^2(\kappa_2)^3}.$$

Figure 13 presents numerical estimates of skewness and excess kurtosis of  $V_1(t)$  obtained from exact cumulant expressions.

As above, our results, which are only proved for non-negative weights, remain accurate although the considered Hawkes process allows for inhibition. In what follows, we use

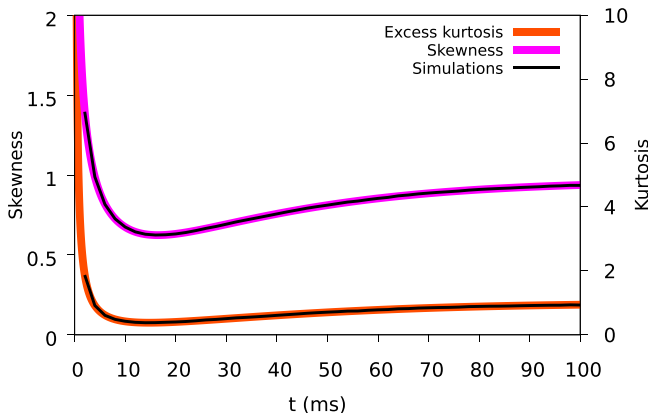


FIG. 13. Skewness and kurtosis of  $V_4(t) = V_1(t)$ .

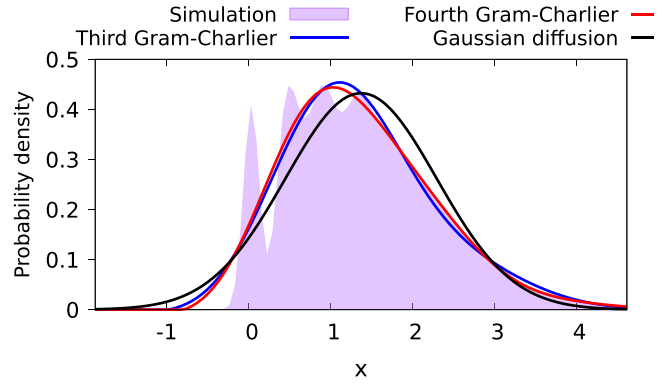


FIG. 14.  $t = 10$  ms.

third- and fourth-order expansions given by

$$\phi_X^{(3)}(x) = \frac{1}{\sqrt{\kappa_2}} \varphi\left(\frac{x - \kappa_1}{\sqrt{\kappa_2}}\right) \left[ 1 + c_3 H_3\left(\frac{x - \kappa_1}{\sqrt{\kappa_2}}\right) \right]$$

and

$$\begin{aligned} \phi_X^{(4)}(x) = & \frac{1}{\sqrt{\kappa_2}} \varphi\left(\frac{x - \kappa_1}{\sqrt{\kappa_2}}\right) \left[ 1 + c_3 H_3\left(\frac{x - \kappa_1}{\sqrt{\kappa_2}}\right) \right. \\ & \left. + c_4 H_4\left(\frac{x - \kappa_1}{\sqrt{\kappa_2}}\right) + c_6 H_6\left(\frac{x - \kappa_1}{\sqrt{\kappa_2}}\right) \right], \end{aligned}$$

and compare them to the first-order expansion

$$\phi_X^{(1)}(x) = \frac{1}{\sqrt{\kappa_2}} \varphi\left(\frac{x - \kappa_1}{\sqrt{\kappa_2}}\right),$$

which corresponds to a Gaussian diffusion approximation. Figures 14 and 15 present second-, third-, and fourth-order Gram-Charlier expansions (5) for the probability density function of the membrane potential  $V_1(t)$ , based on the exact cumulant expressions computed at the times  $t = 10$  ms and  $t = 20$  ms. The purple areas correspond to probability density estimates obtained by Monte Carlo simulations. The second-order expansions correspond to the Gaussian diffusion approximation obtained by matching first- and second-order moments.

Figures 13 and 15 show that the actual probability density estimates obtained by simulation are significantly different from their Gaussian diffusion approximations when skewness and kurtosis take large absolute values. In addition, in Figs. 14

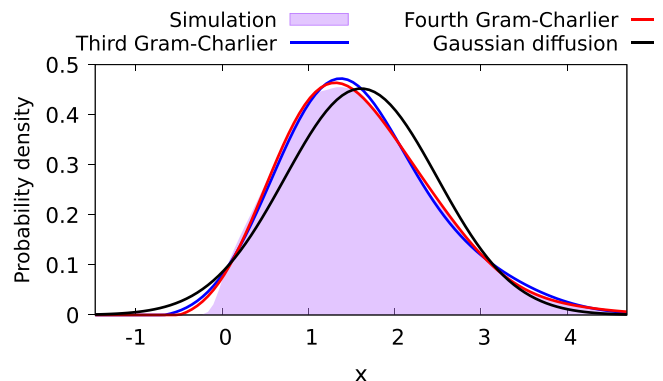


FIG. 15.  $t = 20$  ms.

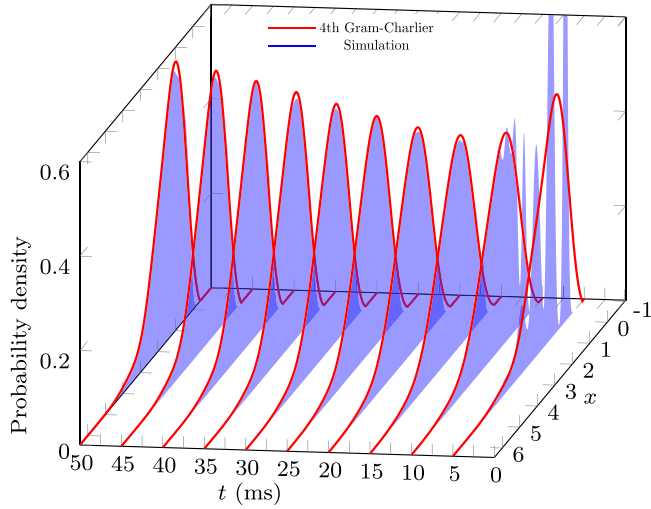


FIG. 16. Fourth-order Gram-Charlier expansions vs simulated densities.

and 15 the fourth-order Gram-Charlier expansions appear to give the best fit to the actual probability densities, which have negative skewness and positive excess kurtosis, see Fig. 13, and the impact of the fourth cumulant remains minimal.

Figure 16 presents time-dependent fourth-order Gram-Charlier expansions (5) based on exact moment formulas at different times for the probability density function of  $V_1(t)$ .

As can be checked from Fig. 16, the fourth-order Gram-Charlier expansions fit the purple areas obtained by Monte Carlo simulations. Figure 17 compares the Gaussian diffusion (blue) approximation to the fourth-order Gram-Charlier expansion (purple) for the probability density function of  $V_1(t)$ , while Fig. 18 represents the relative difference between the Gaussian diffusion and fourth-order approximations.

V. CONCLUSION

This paper presents closed-form expressions for the cumulants of arbitrary orders of filtered multivariate Hawkes processes with excitation and inhibition, for application to the modeling of spike trains. Such expressions can be used for the

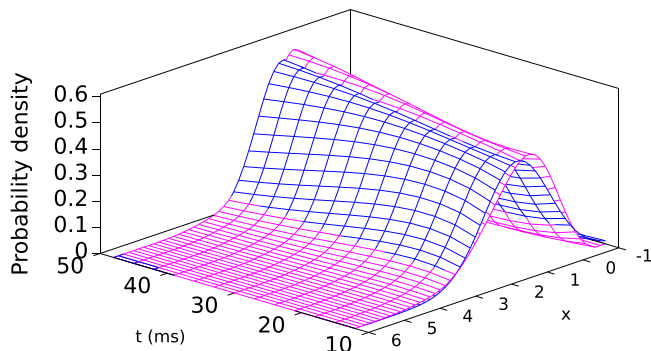


FIG. 17. Gaussian diffusion vs fourth Gram-Charlier expansion.

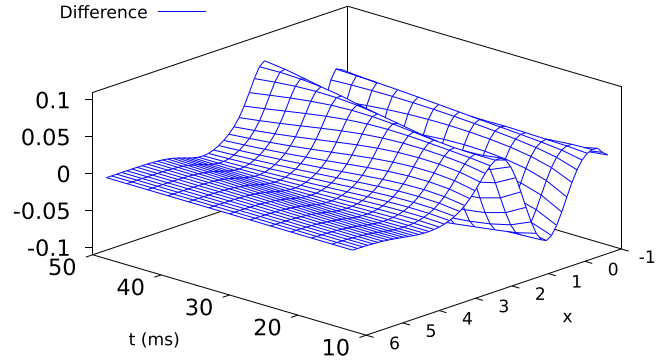


FIG. 18. Difference between second and fourth expansions.

prediction and sensitivity analysis of the statistical behavior of the model over time via immediate numerical evaluations over multiple ranges of parameters, whereas Monte Carlo estimations appear slower and less reliable. They are also used to estimate the probability densities of neuronal membrane potentials using Gram-Charlier density expansions.

ACKNOWLEDGMENT

This research is supported by the Ministry of Education, Singapore, under its Tier 1 Grant No. MOE2020-T1-002-047.

APPENDIX A: PROOFS OF JOINT CUMULANT IDENTITIES

In this section we extend the algorithm of [27,32] for the recursive calculation of the joint cumulants of Hawkes point processes from the univariate to multivariate setting. We consider a self-exciting point process on  $\mathbb{X} := (\mathbb{R}^d) \times \{1, \dots, m\}$ ,  $d \geq 1$ , with Poisson offspring intensities  $\gamma_i(dx \times \{i\}) = \gamma_{i,j}(dx) = \gamma_{i,j}(x)dx$  and Poisson baseline intensity  $\nu(dx \times \{j\}) = \nu_j(dx) = \nu_j(x)dx$  on each copy of  $\mathbb{R}^d$ ,  $j = 1, \dots, m$ . This process is built in the cluster process framework of [28] on the space

$$\Omega = \{\xi = \{(x, i)\}_{i \in I} \subset \mathbb{X} : \#(A \cap \xi) < \infty$$

$$\text{for all compact } A \in \mathcal{B}(\mathbb{X})\}$$

of locally finite configurations on  $\mathbb{X}$ , whose elements  $\xi \in \Omega$  are identified with the Radon point measures  $\xi(dz) = \sum_{(x,i) \in \xi} \epsilon_{(x,i)}(dz)$ , where  $\epsilon_{(x,i)}$  denotes the Dirac measure at  $(x, i) \in \mathbb{X}$ . Any initial point  $(x, i) \in \mathbb{X}$  branches into a Poisson random sample on  $\mathbb{X}$ , denoted by  $\xi_{\gamma_i}^i(dz)$ , with intensity measure  $\gamma_{i,j}(y + dx)$  on every copy of  $\mathbb{R}^d$ ,  $i, j = 1, \dots, m$ . In case  $d = 1$  and  $\gamma_{i,j}(s) = 0$  for  $s \leq 0$ ,

$$N_t^{(i)}(\xi) := \xi([0, t] \times \{i\}) = \sum_{x: (x,i) \in \xi} \mathbf{1}_{[0,t]}(x),$$

$i = 1, \dots, m$ , represents a multivariate Hawkes process with stochastic intensities of the form

$$\lambda_t^{(i)} := \nu + \sum_{j=1}^m \int_0^t \gamma_{i,j}(t-s) dN_s^{(j)},$$

with  $t \in \mathbb{R}_+, i = 1, \dots, m$ . For  $f$  a sufficiently integrable real-valued function on  $\mathbb{X}$ , we let

$$G_{(x,i)}(f) = f(x, i) \mathbb{E}_i \left[ \prod_{(y,j) \in \xi} f(y + x, j) \right]$$

denote the probability generating functional (PGFL) of the branching process  $\xi$  given that it is started from a single point at  $(x, i) \in \mathbb{X}$ . The next proposition states a recursive property for the probability generating functional  $G_{(x,i)}(f)$ ; see also Theorem 1 in [33].

*Proposition 4.* The probability generating functional  $G_{(x,i)}(f)$  satisfies

$$G_{(x,i)}(f) = f(x, i) \exp \left( \sum_{j=1}^m \int_{\mathbb{R}^d} [G_{(x+y,j)}(f) - 1] \gamma_{i,j}(dy) \right),$$

with  $(x, i) \in \mathbb{X}$ , and the PGFL of the Hawkes process with Poisson baseline intensity  $\nu$  on  $\mathbb{X}$  is given by

$$G_\nu(f) = \exp \left( \sum_{i=1}^m \int_{\mathbb{R}^d} [G_{(x,i)}(f) - 1] \nu_i(x) dx \right).$$

*Proof.* Viewing the self-exciting point process  $\xi$  as a marked point process we have, see, e.g., Lemma 6.4.VI of [34],

$$\begin{aligned} G_{(x,i)}(f) &= f(x, i) \mathbb{E}_i \left[ \prod_{(y,j) \in \xi} f(y + x, j) \right] \\ &= f(x, i) \mathbb{E}_i \left[ \prod_{(y,j) \in \xi_{\gamma_j}} \left( \prod_{(z,k) \in \xi} f(z + y + x, k) \right) \right] \\ &= f(x, i) \mathbb{E}_i \left[ \prod_{(y,j) \in \xi_{\gamma_j}} \mathbb{E}_j \left[ \prod_{(z,k) \in \xi} f(x + y + z, k) \right] \right] \\ &= f(x, i) \mathbb{E}_i \left[ \prod_{(y,j) \in \xi_{\gamma_j}} G_{(x+y,j)}(f) \right] \\ &= e^{-\nu(\mathbb{X})} f(x, i) \sum_{n=0}^{\infty} \frac{1}{n!} \sum_{j_1, \dots, j_n=1}^m \int_{(\mathbb{R}^d)^n} \\ &\quad \times G_{(x+y_1, j_1)}(f) \cdots G_{(x+y_n, j_n)}(f) \gamma_{i, j_1}(dy_1) \cdots \gamma_{i, j_n}(dy_n) \\ &= f(x, i) \exp \left( \sum_{j=1}^m \int_{\mathbb{R}^d} [G_{(x+y,j)}(f) - 1] \gamma_{i,j}(dy) \right) \end{aligned}$$

and

$$\begin{aligned} G_\nu(f) &= e^{-\nu(\mathbb{X})} \sum_{n=0}^{\infty} \frac{1}{n!} \sum_{j_1, \dots, j_n=1}^m \int_{(\mathbb{R}^d)^n} \\ &\quad \times G_{(y_1, j_1)}(f) \cdots G_{(y_n, j_n)}(f) \nu_{j_1}(dy_1) \cdots \nu_{j_n}(dy_n) \\ &= \exp \left( \sum_{i=1}^m \int_{\mathbb{R}^d} [G_{(x,i)}(f) - 1] \nu_i(x) dx \right). \end{aligned}$$

Let

$$\begin{aligned} M_{(x,i)}(f) &:= G_{(x,i)}(e^f) \\ &= \mathbb{E}_i \left[ \exp \left( f(x, i) + \sum_{(y,j) \in \xi} f(x + y, j) \right) \right] \end{aligned}$$

denote the moment generating functional (MGFL) of the random sum  $\sum_{(y,j) \in \xi} f(y, j)$  given that the cluster process  $\xi$  starts from a single point at  $(x, i) \in \mathbb{X}$ . The following corollary is an immediate consequence of Proposition 4; see also Proposition 2.6 in [35] for Poisson cluster processes.

*Corollary 5.* The moment generating functional  $M_{(x,i)}(f)$  satisfies the recursive relation

$$M_{(x,i)}(f) = \exp \left( f(x, i) + \sum_{j=1}^m \int_{\mathbb{R}^d} [M_{(x+y,j)}(f) - 1] \gamma_{i,j}(dy) \right), \tag{A1}$$

with  $(x, i) \in \mathbb{X}$ . The MGFL of the Hawkes process with baseline intensity  $\nu$  on  $\mathbb{X}$  is given by

$$M_\nu(f) = \exp \left( \sum_{i=1}^m \int_{\mathbb{R}^d} [M_{(x,i)}(f) - 1] \nu_i(x) dx \right). \tag{A2}$$

*Proof of Proposition 1.* For simplicity, the proof is written using Bell polynomials in the univariate case for  $\kappa_{(x,i)}^{(n)}(f) := \kappa_{(x,i)}^{(n)}(f, \dots, f)$  with  $f = f_1 = \dots = f_n$ , and the general case is deduced by polarization. By (A1), (C1), and the Faà di Bruno formula (C2), we have

$$\begin{aligned} \sum_{n=1}^{\infty} \frac{t^n}{n!} \kappa_{(x,i)}^{(n)}(f) &= \ln M_{(x,i)}(tf) \\ &= tf(x, i) + \sum_{j=1}^m \int_{\mathbb{R}^d} (e^{\ln M_{(x+y,j)}(tf)} - 1) \gamma_{i,j}(dy) \\ &= tf(x, i) + t \sum_{j=1}^m \int_{\mathbb{R}^d} \kappa_{(x+y,j)}^{(1)}(f) \gamma_{i,j}(dy) \\ &\quad + \sum_{n=2}^{\infty} \frac{t^n}{n!} \sum_{j=1}^m \int_{\mathbb{R}^d} B_n(\kappa_{(x+y,j)}^{(1)}(f), \dots, \kappa_{(x+y,j)}^{(n)}(f)) \gamma_{i,j}(dy). \end{aligned} \tag{A3}$$

At the first order, the expansion (A3) yields

$$\begin{aligned} \kappa_{(x,i)}^{(1)}(f) &= f(x, i) + \int_{\mathbb{R}^d} \sum_{j=1}^m \kappa_{(x+y,j)}^{(1)}(f) \gamma_{i,j}(dy) \\ &= f(x, i) + \sum_{n=1}^{\infty} \sum_{j_1, \dots, j_n=1}^m \int_{\mathbb{R}^d} \cdots \int_{\mathbb{R}^d} \\ &\quad \times f(x + y_1 + \dots + y_n, j_n) \gamma_{i, j_2}(dy_1) \cdots \gamma_{j_{n-1}, j_n}(dy_n), \end{aligned}$$

while at the order  $n \geq 2$  it shows that

$$\begin{aligned} \kappa_{(x,i)}^{(n)}(f) &= \sum_{j=1}^m \int_{\mathbb{R}^d} B_n(\kappa_{(x+y,i)}^{(1)}(f), \dots, \kappa_{(x+y,i)}^{(n)}(f)) \gamma_{i,j}(dy) \\ &= [\Gamma \kappa_{(\cdot, \cdot)}^{(n)}(f)](x, i) \\ &\quad + \{ \Gamma [B_n(\kappa_{(\cdot, \cdot)}^{(1)}(f), \dots, \kappa_{(\cdot, \cdot)}^{(n)}(f)) - \kappa_{(\cdot, \cdot)}^{(n)}(f)] \}(x, i). \end{aligned}$$

■



The above relation rewrites as

$$\begin{aligned} & [(I - \Gamma)\kappa_{(\cdot, \cdot)}^{(n)}(f)](x, i) \\ &= \Gamma[B_n(\kappa_{(\cdot, \cdot)}^{(1)}(f), \dots, \kappa_{(\cdot, \cdot)}^{(n)}(f)) - \kappa_{(\cdot, \cdot)}^{(n)}(f)](x, i), \end{aligned}$$

which yields

$$\begin{aligned} & \kappa_{(x, i)}^{(n)}(f) \\ &= \{(I - \Gamma)^{-1}\Gamma[B_n(\kappa_{(\cdot, \cdot)}^{(1)}(f), \dots, \kappa_{(\cdot, \cdot)}^{(n)}(f)) - \kappa_{(\cdot, \cdot)}^{(n)}(f)]\}(x, i) \\ &= \sum_{p=1}^{\infty} \sum_{i_1, \dots, i_p=1}^m \int_{\mathbb{R}^d} \dots \int_{\mathbb{R}^d} \\ & \quad \times [B_n(\kappa_{(x+x_1+\dots+x_p, i_p)}^{(1)}(f), \dots, \kappa_{(x+x_1+\dots+x_p, i_p)}^{(n)}(f)) \\ & \quad - \kappa_{(x+x_1+\dots+x_p, i_p)}^{(n)}(f)] \gamma_{i, i_1}(dx_1) \dots \gamma_{i_{p-1}, i_p}(dx_p) \\ &= \sum_{p=1}^{\infty} \sum_{i_1, \dots, i_p=1}^m \sum_{k=2}^n \int_{\mathbb{R}^d} \dots \int_{\mathbb{R}^d} \\ & \quad \times B_{n, k}(\kappa_{(x+x_1+\dots+x_p, i_p)}^{(1)}(f), \dots, \kappa_{(x+x_1+\dots+x_p, i_p)}^{(n-k+1)}(f)) \\ & \quad \times \gamma_{i, i_1}(dx_1) \dots \gamma_{i_{p-1}, i_p}(dx_p), \end{aligned}$$

$n \geq 2$ . ■

*Proof of Corollary 2.*

As above, the proof is only written using Bell polynomials in the case  $f = f_1 = \dots = f_n$ . By (C1), (A2), and the Faà di Bruno formula (C2), we have

$$\begin{aligned} & \sum_{n=1}^{\infty} \frac{t^n}{n!} \kappa^{(n)}(f) = \ln M_v(tf) \\ &= \sum_{i=1}^m \int_{\mathbb{R}^d} [M_{(x, i)}(tf) - 1] v_i(x) dx \\ &= \sum_{i=1}^m \int_{\mathbb{R}^d} (e^{\ln M_{(x, i)}(tf)} - 1) v_i(x) dx \\ &= \sum_{i=1}^m \sum_{n=1}^{\infty} \frac{t^n}{n!} B_n(\kappa_{(x, i)}^{(1)}(f), \dots, \kappa_{(x, i)}^{(n)}(f)) v_i(x) dx, \end{aligned}$$

and therefore

$$\kappa^{(n)}(f) = \sum_{i=1}^m \int_{\mathbb{R}^d} B_n(\kappa_{(x, i)}^{(1)}(f), \dots, \kappa_{(x, i)}^{(n)}(f)) v_i(x) dx,$$

$n \geq 2$ . ■

*Proof of Lemma 3.* Here we take  $d = 1$ . For all  $p, \eta \geq 0$  we have the equalities

$$\begin{aligned} & [(I - \Gamma)^{-1}\Gamma e_{p, \eta, t, k}](x, i) \\ &= \sum_{n=1}^{\infty} \sum_{j_1, \dots, j_{n-1}=1}^m \int_{[0, t]^n} e_{p, \eta, t, k}(x + x_1 + \dots + x_n) \\ & \quad \times \gamma_{i, j_1}(dx_1) \dots \gamma_{j_{n-1}, k}(dx_n) \end{aligned}$$

$$\begin{aligned} &= \sum_{n=1}^{\infty} \frac{[W^n]_{i, k}}{(n-1)!} \int_0^{t-x} (x+y)^p e^{\eta(x+y)} y^{n-1} e^{-by} dy \\ &= e^{\eta x} \int_0^{t-x} (x+y)^p [W e^{yW}]_{i, k} e^{(\eta-b)y} dy \\ &= \int_0^{t-x} e_{p, \eta, t, k}(x+y) [W e^{yW}]_{i, k} e^{-by} dy, \quad x \in [0, t], \end{aligned}$$

where we used the fact that the sum  $\tau_1 + \dots + \tau_n$  of  $n$  exponential random variables with parameter  $b > 0$  has a gamma distribution with shape parameter  $n \geq 1$  and scaling parameter  $b > 0$ . ■

### APPENDIX B: COMPUTER CODES

The recursion (2) and Eq. (3) can be implemented for any family  $(g_1, \dots, g_n)$  of functions defined on  $\mathbb{R}_+$  in the following MAPLE code. The joint cumulants  $\langle\langle V_{l_1}(t_1) \dots V_{l_n}(t_n) \rangle\rangle$  are obtained for  $1 \leq l_1, \dots, l_n \leq m$  using the command `c(W, b, g1, ..., gn, l1, ..., ln, t1, ..., tn, mu)` in the code below:

```
with(LinearAlgebra):
a := proc(y) option remember; return evalf(Multiply(W,
MatrixExponential(W, y))); end proc;
h := proc(z, j, W, b, g::list, l::list, t::list) local p, q,
r, s, y, i, m, n, k, c; option remember; n := nops(t);
if n = 1 then return evalf(g[l](z,
t[1]*charfcn[j](1[t1]) + int(g[l](z + y,
t[1]*exp(-b*y)*a(y)[j, 1[t1]], y = 0.. t[1] - z))); end
if; s := 0; r := Iterator:-SetPartitions(n); for q in r
do p := r:-ToSets(q); if 2 <= nops(p) then for k to
Dimension(W)[1] do c := exp(-b*y)*a(y)[j, k]; for i to
nops(p) do c := c*h(z + y, k, W, b, map(op,
convert(p[i], list), g), map(op, convert(p[i], list),
l), map(op, convert(p[i], list), t))); end do; s := s +
c; end do; end if; end do; return int(s, y = 0.. t[1] -
z); end proc;
c := proc(W, b, g::list, l::list, t::list, mu::list) local
y, e, p, q, r, s, i, j, m, n; option remember; n :=
nops(t); s := 0; for j to Dimension(W)[1] do s := s +
mu[j](y)*h(y, j, W, b, g, l, t); if 2 <= n then r :=
Iterator:-SetPartitions(n); for q in r do p :=
r:-ToSets(q); if 2 <= nops(p) then e := 1; for i to
nops(p) do e := e*h(y, j, W, b, map(op, convert(p[i],
list), g), map(op, convert(p[i], list), l), map(op,
convert(p[i], list), t))); end do; s := s + mu[j](y)*e;
end if; end do; end if; return s; end proc;
```

Joint moments can be computed in MAPLE using the command `m(W, b, g1, ..., gn, j1, ..., j1, t1, ..., tn, mu)` defined in the following code:

```
m := proc(W, b, f::list, l::list, t::list, mu::list) local
e, u, p, q, r, s, i, n; option remember; n := nops(t);
s := c(W, b, f, l, t, mu); if 2 <= n then r :=
Iterator:-SetPartitions(n); for q in r do p :=
r:-ToSets(q); if 2 <= nops(p) then e := 1; for i to
nops(p) do e := e*c(W, b, map(op, convert(p[i], list),
f), map(op, convert(p[i], list), l), map(op,
convert(p[i], list), t), mu); end do; s := s + e; end
if; end do; end if; return s; end proc;
```

Alternatively, the computation of joint cumulants can be carried out using the command

$c[W, b, \{g_1, \dots, g_n\}, \{l_1, \dots, l_n\}, \{t_1, \dots, t_n\}, \mu]$  in the following MATHEMATICA codes:

```
Needs["Combinatorica`"]
a[y_] := W . MatrixExp[y*W];
h[z_, j_Integer, W_, b_, g_, l_, t_] := h[z, j, W, b, g,
  l, t] = (Module[{y, k, i, c, n, m, s}, n = Length[t];
  If[n == 1, Return[g[[1]][z, t[[1]]*Boole[j == 1[[1]]]
  + Integrate[g[[1]][z + y, t[[1]]*E^(-b*y)*a[y][[j,
  l[[1]]], {y, 0, t[[1] - z}]]; s = 0; Do[c = 1;
  If[Length[p] >= 2, For[i = 1, i <= Length[p], i++, c =
  Block[{u = y + z, w = g[[p[[i]]]], r = 1[[p[[i]]]], v =
  t[[p[[i]]]], h[u, k, W, b, w, r, v]]; s += c], {p,
  SetPartitions[n]}];
  Return[Sum[Integrate[E^(-b*y)*a[y][[j, k]]*s, {y, 0,
  t[[1] - z}], {k, 1, Dimensions[W][[1]]}]]];
c[W_, b_, g_, l_, t_, mu_] := (Module[{y, e, n, i, j, m,
  s}, n = Length[g]; s = 0; For[j = 1, j <=
  Dimensions[W][[1]], j++, Do[e = mu[y][[j]]; For[i = 1,
  i <= Length[p], i++, e = Block[{u = y, w =
  g[[p[[i]]]], r = 1[[p[[i]]]], v = t[[p[[i]]]], h[u, j,
  W, b, w, r, v]]; s += Flatten[{e}][[1]], {p,
  SetPartitions[n]}]; Return[Integrate[s, {y, 0,
  t[[1]]}]]];
```

Figures 3–10 can also be plotted from the following MATHEMATICA commands:<sup>1</sup>

```
W := {{10, 0, 10, 0}, {0, 10, 10, -8}, {10, 10, 0, -8}, {10,
  10, 10, -10}};
g[u_, t_] := E^(-(t - u)/0.01); mu[t_] := {250, 250, 250,
  250};
c[W, 50, {g}, {2}, {t}, mu] (*First cumulant of V2(t) -
  comp. time one second*)
c[W, 50, {g,g}, {4,4}, {t,t}, mu] (*Second cumulant of V4(t)
  - comp. time 122 seconds*)
c[W, 50, {g,g}, {4,2}, {t,0.05}, mu] (*Covariance of
  (V2(t1),V4(t)) for t<t1=0.05 - comp. time 250 seconds*)
c[W, 50, {g,g}, {2,4}, {0.05,t}, mu] (*Covariance of
  (V2(t1),V4(t)) for t>t1=0.05 - comp. time 250 seconds*)
c[W, 50, {g,g,g}, {4,4,4}, {t,t,t}, mu] (*Third cumulant of
  V4(t) - comp. time 3057 seconds*)
c[W, 50, {g,g,g}, {4,1,1}, {t,0.05,0.05}, mu] (*Third joint
  cumulant of (V1(t1),V1(t1),V4(t)), t<t1=0.05*)
c[W, 50, {g,g,g}, {1,1,4}, {0.05,0.05,t}, mu] (*Third joint
  cumulant of (V1(t1),V1(t1),V4(t)), t>t1=0.05*)
c[W, 50, {g,g,g,g}, {4,4,4,4}, {t,t,t,t}, mu] (*Fourth
  cumulant of V4(t)*)
c[W, 50, {g,g,g,g}, {1,2,3,4}, {t,t,t,t}, mu] (*Fourth joint
  cumulant of (V1(t),V2(t),V3(t),V4(t))*
```

Standard moments of order  $n \geq 1$  can be computed in MATHEMATICA using the command  $m[W, b, \{g_1, \dots, g_n\}, \{l_1, \dots, l_n\}, \{t_1, \dots, t_n\}, \mu]$  defined below:

```
m[W_, b_, g_, l_, t_, mu_] := (Module[{n, e, i, s}, s =
  0; n = Length[t]; If[n == 0, Return[1]]; Do[e = 1;
  For[i = 1, i <= Length[pp], i++, e = c[W, b,
  g[[pp[[i]]]], l[[pp[[i]]]], t[[pp[[i]]]], mu]]; s += e,
  {pp, SetPartitions[n]}]; Flatten[{s}][[1]]];
```

The codes listed in this section are available for download as a MAPLE worksheet and MATHEMATICA notebook; see [36].

### APPENDIX C: JOINT CUMULANTS AND FAÀ DI BRUNO FORMULA

We refer to, e.g., Ref. [37] or [38] for the background combinatorics recalled in this section. The joint cumulants

of orders  $(l_1, \dots, l_n)$  of a random vector  $X = (X_1, \dots, X_n)$ ,  $1 \leq l_1, \dots, l_n \leq m$ , are the coefficients  $\langle\langle X_1^{l_1} \dots X_n^{l_n} \rangle\rangle$  appearing in the log-moment generating (MGF) expansion

$$\ln\langle e^{t_1 X_1 + \dots + t_n X_n} \rangle = \sum_{l_1, \dots, l_n \geq 1} \frac{t_1^{l_1} \dots t_n^{l_n}}{l_1! \dots l_n!} \langle\langle X_1^{l_1} \dots X_n^{l_n} \rangle\rangle, \quad (C1)$$

for  $(t_1, \dots, t_n)$  in a neighborhood of zero in  $\mathbb{R}^n$ . Recall that if  $f(t)$  admits the formal series expansion

$$f(t) = \sum_{n=1}^{\infty} \frac{a_n}{n!} t^n,$$

by the Faà di Bruno formula we have

$$e^{f(t)} - 1 = \sum_{n=1}^{\infty} \frac{t^n}{n!} B_n(a_1, \dots, a_n), \quad (C2)$$

where

$$B_n(a_1, \dots, a_n) = \sum_{k=1}^n B_{n,k}(a_1, \dots, a_{n-k+1})$$

is the complete Bell polynomial of degree  $n \geq 1$  and

$$B_{n,k}(a_1, \dots, a_{n-k+1}) = \sum_{\pi_1 \cup \dots \cup \pi_k = \{1, \dots, n\}} a_{|\pi_1|}(X) \dots a_{|\pi_k|}(X),$$

where  $1 \leq k \leq n$ , is the partial Bell polynomial of order  $(n, k)$ , where the sum runs over the partitions  $\pi_1, \dots, \pi_k$  of the set  $\{1, \dots, n\}$  and  $|\pi_i|$  denotes the cardinality of  $\pi_i$ . Joint moments can be obtained from the joint moment-cumulant relation

$$\langle V_{l_1}(t_1) \dots V_{l_n}(t_n) \rangle = \sum_{\pi \in \Pi[n]} \prod_{j=1}^{|\pi|} \left\langle\left\langle \prod_{i \in \pi_j} V_{l_i}(t_i) \right\rangle\right\rangle, \quad (C3)$$

where the above sum is over the set  $\Pi[n]$  of partitions  $\pi$  of  $\{1, \dots, n\}$ . Joint cumulants can also be recovered from joint moments from the relation

$$\langle\langle V_{l_1}(t_1) \dots V_{l_n}(t_n) \rangle\rangle = \sum_{\pi \in \Pi[n]} (|\pi| - 1)! (-1)^{|\pi|-1} \prod_{j=1}^{|\pi|} \left\langle \prod_{i \in \pi_j} V_{l_i}(t_i) \right\rangle,$$

where the above sum is over the set  $\Pi[n]$  of partitions  $\pi$  of  $\{1, \dots, n\}$ , which can be obtained by Möbius inversion of the moment-cumulant relation (C3).

<sup>1</sup>MATHEMATICA computation times are significantly higher, probably due to the way recursions are carried out.

- [1] A. Hawkes, Spectra of some self-exciting and mutually exciting point processes, *Biometrika* **58**, 83 (1971).
- [2] S. Cardanobile and S. Rotter, Multiplicatively interacting point processes and applications to neural modeling, *J. Comput. Neurosci.* **28**, 267 (2010).
- [3] M. Krumin, I. Reutsky, and S. Shoham, Correlation-based analysis and generation of multiple spike trains using Hawkes models with an exogenous input, *Front. Comput. Neurosci.* **4**, 12 (2010).
- [4] F. Gerhard, M. Deger, and W. Truccolo, On the stability and dynamics of stochastic spiking neuron models: Nonlinear Hawkes process and point process GLMs, *PLoS Comput. Biol.* **13**, e1005390 (2017).
- [5] Y. Chen, Q. Xin, V. Ventura, and R. E. Kass, Stability of point process spiking neuron models, *J. Comput. Neurosci.* **46**, 19 (2019).
- [6] P. Reynaud-Bouret, V. Rivoirard, and C. Tuleau-Malot, Inference of functional connectivity in neurosciences via Hawkes processes, in *2013 IEEE Global Conference on Signal and Information Processing* (IEEE Press, New York, 2013), pp. 317–320.
- [7] G. Ocker, K. Josić, E. Shea-Brown, and M. Buice, Linking structure and activity in nonlinear spiking networks, *PLoS Comput. Biol.* **13**, e1005583 (2017).
- [8] M. Kordovan and S. Rotter, Spike train cumulants for linear-nonlinear Poisson cascade models, [arXiv:2001.05057](https://arxiv.org/abs/2001.05057).
- [9] A. Verveen and L. DeFelice, Membrane noise, *Prog. Biophys. Mol. Biol.* **28**, 189 (1974).
- [10] H. Tuckwell, *Introduction to Theoretical Neurobiology: Volume 2, Nonlinear and Stochastic Theories* (Cambridge University Press, Cambridge, UK, 1988).
- [11] A. Kuhn, A. Aertsen, and S. Rotter, Neuronal integration of synaptic input in the fluctuation-driven regime, *J. Neurosci.* **24**, 2345 (2004).
- [12] M. Rudolph and A. Destexhe, An extended analytic expression for the membrane potential distribution of conductance-based synaptic noise, *Neural Comput.* **17**, 2301 (2005).
- [13] M. Richardson and W. Gerstner, Synaptic shot noise and conductance fluctuations affect the membrane voltage with equal significance, *Neural Comput.* **17**, 923 (2005).
- [14] A. N. Burkitt, A review of the integrate-and-fire neuron model: I. Homogeneous synaptic input, *Biol. Cybern.* **95**, 1 (2006).
- [15] L. Wolff and B. Lindner, Method to calculate the moments of the membrane voltage in a model neuron driven by multiplicative filtered shot noise, *Phys. Rev. E* **77**, 041913 (2008).
- [16] L. Wolff and B. Lindner, Mean, variance, and autocorrelation of subthreshold potential fluctuations driven by filtered conductance shot noise, *Neural Comput.* **22**, 94 (2010).
- [17] K.-I. Amemori and S. Ishii, Gaussian process approach to spiking neurons for inhomogeneous Poisson inputs, *Neural Comput.* **13**, 2763 (2001).
- [18] A. N. Burkitt, A review of the integrate-and-fire neuron model: II. Inhomogeneous synaptic input and network properties, *Biol. Cybern.* **95**, 97 (2006).
- [19] D. Cai, L. Tao, A. Rangan, and D. W. McLaughlin, Kinetic theory for neuronal network dynamics, *Commun. Math. Sci.* **4**, 97 (2006).
- [20] M. Brigham and A. Destexhe, Nonstationary filtered shot-noise processes and applications to neuronal membranes, *Phys. Rev. E* **91**, 062102 (2015).
- [21] N. Privault, Nonstationary shot-noise modeling of neuron membrane potentials by closed-form moments and Gram-Charlier expansions, *Biol. Cybern.* **114**, 499 (2020).
- [22] A. Dassios and H. Zhao, A dynamic contagion process, *Adv. Appl. Probab.* **43**, 814 (2011).
- [23] L. Cui, A. Hawkes, and H. Yi, An elementary derivation of moments of Hawkes processes, *Adv. Appl. Probab.* **52**, 102 (2020).
- [24] A. Daw and J. Pender, Matrix calculations for moments of Markov processes, *Adv. Appl. Probab.* (to be published), [arXiv:1909.03320](https://arxiv.org/abs/1909.03320).
- [25] E. Bacry, K. Dayri, and J. Muzy, Non-parametric kernel estimation for symmetric Hawkes processes. Application to high frequency financial data, *Eur. Phys. J. B* **85**, 157 (2012).
- [26] S. Jovanović, J. Hertz, and S. Rotter, Cumulants of Hawkes point processes, *Phys. Rev. E* **91**, 042802 (2015).
- [27] N. Privault, Recursive computation of the Hawkes cumulants, *Statist. Probab. Lett.* **177**, article 109161 (2021).
- [28] A. Hawkes and D. Oakes, A cluster process representation of a self-exciting process, *J. Appl. Probab.* **11**, 493 (1974).
- [29] Y. Ogata, On Lewis' simulation method for point processes, *IEEE Trans. Inf. Theory* **27**, 23 (1981).
- [30] Y. Chen (unpublished).
- [31] H. Cramér, *Mathematical Methods of Statistics* (Princeton University Press, Princeton, NJ, 1946), pp. x+545.
- [32] N. Privault, An algorithm for the computation of joint Hawkes moments with exponential kernel, in *Proceedings of the 53rd ISCTE International Symposium on Stochastic Systems Theory and Its Applications (SSS'21)* (The Institute Of Systems, Control And Information Engineers, 2022), Vol. 2022, pp. 72–79.
- [33] L. Adamopoulos, Some counting and interval properties of the mutually-exciting processes, *J. Appl. Probab.* **12**, 78 (1975).
- [34] D. J. Daley and D. Vere-Jones, *An Introduction to the Theory of Point Processes. Vol. I, Probability and its Applications* (Springer-Verlag, New York, 2003), pp. xxii+469.
- [35] L. Bogachev and A. Daletskii, Poisson cluster measures: Quasi-invariance, integration by parts and equilibrium stochastic dynamics, *J. Funct. Anal.* **256**, 432 (2009).
- [36] See Supplemental Material at <http://link.aps.org/supplemental/10.1103/PhysRevE.106.054410> for the MAPLE and MATHEMATICA codes mentioned in the paper.
- [37] E. Lukacs, Applications of Faà di Bruno's formula in mathematical statistics, *Amer. Math. Monthly* **62**, 340 (1955).
- [38] P. McCullagh, *Tensor Methods in Statistics*, Monographs on Statistics and Applied Probability (Chapman & Hall, London, 1987), pp. xvi+285.